

Histopathology and ultrastructural alterations in gastric mucus-secreting cells in diabetic model rats

Sani Baimai^{1,2}, Sirinush Sricharoenvej², Passara Lanlua², Narawadee Choompoo¹

¹ Department of Anatomy, Faculty of Medical Science, Naresuan University, Phitsanulok, 65000, Thailand

² Department of Anatomy, Faculty of Medicine Siriraj Hospital, Mahidol University, Bangkok, 10700, Thailand

SUMMARY

Diabetes mellitus (DM) can cause gastric ulcers (GU), duodenal ulcers (DU), and gastroesophageal reflux disease (GERD). Mucus-secreting cells secrete mucus, which aids in the neutralization of HCl and inhibits bacteria. DM can alter mucus-secreting cells. Due to a lack of mucosal defense, external stimuli such as bacteria or ethanol can lead to the development of GU, DU, and GERD. This research study used a STZ-induced diabetic rat model to examine the short- and long-term histopathology and ultrastructural alterations in mucus-secreting cells in the cardia, body, and pyloric regions of the stomach. Quantitative analysis was also employed in this study to examine the distribution of mucin granules across all three locations. Twenty-four male adult Sprague-Dawley rats were utilized. Rats were divided into the control (n = 12) and DM (n = 12) groups. Each was separated into short-term (4 weeks) and long-term (24 weeks) rats. For DM induction, streptozotocin (STZ) can selectively destroy the beta cells of the pancreas. The DM was injected with STZ in citrate buffer at 60 mg/kg body weight. The control group was injected with citrate buffer. Histopathology was examined by Alcian blue-Periodic Acid Schiff

staining under a light microscope. Image analysis was applied to quantify mucin accumulation. The ultrastructure was explored using transmission electron microscopy. In short-term and long-term DM, there was superficial erosion of the gastric epithelium and a significant decrease in the percentage of mucin granule accumulations in both surface mucous cells (SMCs) and mucous neck cells (MNCs). In short-term DM, SMCs were degenerated with vacuolation, disrupted cristae of mitochondria, and dilated rough endoplasmic reticulum (rER). MNCs were swollen with destroyed organelles. In long-term DM, degenerative nuclei and electron-lucent regions with unidentified structures of SMCs were observed. Nuclear chromatin condensation and the disappearance of mucin granules were present in MNCs. In conclusion, under both LM and TEM, STZ-induced diabetic rats demonstrated both short- and long-term damage to the gastric mucosa and gastric gland structures.

Key words: Surface mucous cells – Mucous neck cells – Stomach – Streptozotocin – Ultrastructure – Mucin granules

Corresponding author:

Narawadee Choompoo, Ph.D. Department of Anatomy, Faculty of Medical Science, Naresuan University, Phitsanulok, 65000, Thailand. Phone: (+66) 95-635-9305. E-mail: narawadeec@nu.ac.th

Submitted: June 5, 2023. Accepted: July 23, 2023

<https://doi.org/10.52083/BIHZ6841>

INTRODUCTION

Diabetes mellitus (DM) is a metabolic syndrome that is increasing worldwide. DM can be diagnosed based on a persistent high blood glucose level and HbA1c of more than 126 mg/dL and 6.5%, respectively. DM can be classified into two main categories: type 1 (T1DM, absolute insulin deficiency) and type 2 (T2DM, insulin resistance and relative insulin decrease) (Krishnan et al., 2013). DM has been reported to lead to several diabetes-related complications, such as diabetic neuropathy, diabetic endocrinology, and gastrointestinal symptoms (Baimai et al., 2020, 2021; Lerkdumnerkit et al., 2022). Diabetic patients with diabetic gastropathy (75%) appear to have many gastric symptoms, such as epigastric pain, nausea, vomiting, weight loss, abdominal bloating, postprandial fullness, hematemesis, and hematochezia (Sabatine, 2020). All of these symptoms are related to gastric ulcer (GU), duodenal ulcer (DU), and gastroesophageal reflux disease (GERD).

Gastric mucosal secretory cells play an essential role in the stomach secreting mucous to protect the gastric epithelium (Barrett et al., 2010). Mucus-secreting cells are composed of surface mucous (SMCs) and mucous neck (MNCs) cells of the gastric mucosa and gastric gland, which are an essential part of mucosal protection. SMCs and MNCs secrete mucus-containing alkaline bicarbonate (HCO_3), which aids in the neutralization of HCl and inhibits bacteria (Barrett et al., 2010). DM can alter mucus-secreting cells, which leads to impaired protective defense. Gastric mucosal lesions in DM, for example, mucosal hyperemia, desquamation of surface epithelium, foci of mucosal necrosis and erosion, and decreased mucus-secreting cells, have been reported (Raafat et al., 2019). GU occurs when there is an imbalance between mucosal protection and gastric acid destruction. Reduced mucus containing alkaline bicarbonate (HCO_3) from the gastric mucosa and gastric gland proper, which is located in the stomach's body, can reduce the factor inhibiting bacteria. As a result, external factors such as *H. pylori*, drugs such as NSAIDs, and ethanol can easily cause GU. All those external factors can pass from the stomach to the duodenum if the mucus-secreting cells in the pyloric mucosa and pyloric gland are reduced.

These factors also consequently cause DU. In addition, decreased mucus-secreting cells at the cardiac part of the stomach allow acid to revert up into the esophagus, causing GERD.

The histopathology and ultrastructural changes in diabetic mucus-secreting cells in the mucosal and glandular regions have never been published, and it would be interesting to investigate the short- and long-term histopathology and ultrastructural changes in mucus-secreting cells in the cardia, body, and pyloric regions of the stomach in a STZ-induced diabetic disease rat model. This study also used quantitative analysis to compare the proportion of mucin granules in each area in all three regions. The results of this research can confirm the histopathological evidence and ultrastructural damage using various techniques to relate the cause of DM with cell damage and gastric symptoms. These discoveries could lead to the development of diagnostic strategies, preventive awareness, and treatments for DM.

MATERIALS AND METHODS

Animal model

Twenty-four male adult Sprague-Dawley rats (6-8 weeks old), weighing between 200-230 g, were employed. All animals were obtained from the National Laboratory Animal Center at Mahidol University in Thailand. The "Guide for the Care and Use of Laboratory Animals" was followed when caring for the animals used in this investigation, which was authorized by the Siriraj Animal Care and Use Protocol at Mahidol University in Thailand (COA No. 001/2564). Each animal was housed in a tidy individual cage and exposed to a set routine for temperature (25°C), illumination (12:12-hour light: dark cycle with the lights on at 7 a.m.), humidity (55±10%), and ventilation (15-20 times per hour). Throughout the trial, the animals had access to water and a standard laboratory food ad libitum (Baimai et al., 2020, 2021; Chookliang et al., 2021; Lerkdumnerkit et al., 2022).

Drug and animal induction

The rats were randomly divided into the control and DM groups that had been injected with streptozotocin (STZ) (Across Organics, Janssen

Pharmaceutical, Belgium) to induce DM. Twelve rats from the diabetic group received a single intraperitoneal injection of STZ at a dose of 60 mg/kg body weight in citrate buffer at pH 4.5 (Baimai et al., 2020, 2021; Chookliang et al., 2021; Lerkdumnernkit et al., 2022). The same amount of the buffer was intraperitoneally administered to 12 rats in the age-matched control group. As short- and long-term outcomes, all animals were slaughtered 4 and 24 weeks following intraperitoneal injection, respectively.

Measurement of glucose concentration before the experiment and after STZ induction

Each animal was subjected to a 7-day fast, during which time the amount of glucose in their urine was measured using urinalysis control strips (Diabur-Test 5000, Roche Ltd., Germany). Glucose strips (One Touch® Ultra®, USA) were used to measure the entire blood glucose in a blood sample that was also drawn from the tail vein. Animals were used in this experiment if the urine glucose concentration was 0 mg/dL and the whole blood glucose level was less than 300 mg/dL (Baimai et al., 2020, 2021; Chookliang et al., 2021; Lerkdumnernkit et al., 2022). After a 12-hour fast, the body weight, and urine glucose levels were checked each day. After STZ administration at 48 hours, 72 hours, and before sacrifice, whole-blood glucose levels were collected and assessed.

Histopathological study

A histopathological examination using light microscopy (LM) was conducted on six control and six STZ-induced diabetic rats in each period. Before the thoracic cage was dissected to reveal the heart, each animal was sedated by inhaling halothane. Immediately after that, 0.05 ml of heparin was administered into the left ventricle and allowed to circulate for 1-2 minutes to stop blood coagulation. The ascending aorta was accessed through the left ventricle with a blunt needle (18 gauge), which was then constricted tightly. To allow the outflow of the perfused blood, the right atrium was then severed. The animal received 500 ml of a 0.9% NaCl solution through the same catheter to flush the blood out of the circulation. The treatment was carried out following the needs of

each group of animals until the outflow fluid was clear. To preserve the tissues after perfusion with 0.1 M phosphate buffer solution (PBS), 2.5% glutaraldehyde in 0.1 M PBS was manually administered into the ascending aorta (Baimai et al., 2020, 2021; Chookliang et al., 2021; Lerkdumnernkit et al., 2022;). The abdominal wall was surgically incised and opened after that. The stomach was then removed, cut open along the larger curvature, and left in the same fixative overnight.

The stomach was dissected from each region using a sharp blade. In the histopathological study, the stomach was serially sectioned at a thickness of 5 µm. SMCs and MNCs were stained using Alcian blue-Periodic Acid Schiff (PAS) to detect mucin. Under a light microscope attached to a digital camera, all specimens were examined and captured with a camera (AxioCam MRC, Jena, Germany). Small portions of the stomach (1 mm³) in each location were postfixed in 1% osmium tetroxide in 0.1 M PBS before being cut into plastic blocks using an ultramicrotome; the plastic specimens were serially sectioned at 1-1.5 µm thickness (Leica EM UC6, Vienna, Austria) (Baimai et al., 2020, 2021; Chookliang et al., 2021; Lerkdumnernkit et al., 2022).

The mucin granule accumulations

Combined Alcian-blue and PAS staining was used to detect the mucin of SMCs and MNCs separately. The PAS-positive reaction can be used to locate the mucin of SMCs in addition to cell location. The MNCs, on the other hand, can be identified by a strong Alcian blue-positive reaction. Ninety sections per group were chosen to quantify mucin-stained mucus-secretory cell depositions, which were calculated as the percentage of mucin per area at 20x magnification. All quantitative data were counted, measured, calculated, and analyzed by using the ImageJ software tool (National Institute of Mental Health, Bethesda, Maryland, USA).

Ultrastructural study

Post-fixation of small sections of the stomach (1 mm³) in 1% osmium tetroxide in 0.1 M PBS was followed by drying in a graded series of ethanol, cleaning in propylene oxide, and infiltration by

propylene oxide. The specimens were then implanted in plastic. An ultramicrotome (Leica EM UC6, Vienna, Austria) was used to section the tissue blocks. Semithin sections (1-1.5 μm) were stained with toluidine blue and examined under LM for representative areas (Axiostar plus, Jena, Germany). The ultramicrotome was then used to serially section the selected embedded specimens at 80-85 nm thickness. Then, 1% uranyl acetate and lead citrate were used to stain the serial sections (Baimai et al., 2020, 2021; Chookliang et al., 2021; Lerkdumnerkit et al., 2022). Under the TEM, the ultrastructure of the stomach was viewed and photographed (TECNI20, Phillips Electron Optics, Holland).

Statistical analysis

The data were calculated as the mean \pm standard deviation (SD). Differences between independent groups were analyzed by using the independent

t-test (SPSS version 20.0 software, Inc., Chicago, IL, USA). Differences were considered significant at a p -value < 0.05 .

RESULTS

Diabetic rats exhibited symptoms such as polyuria, polydipsia, and polyphagia. Long-term diabetic rats had more severe symptoms than short-term diabetic rats. Most diabetic rats were lethargic, tended to sleep, were not active, and had grooming drops. Generalized myopathy with weight loss was significantly presented in diabetic rats [short-term control = 325.18 ± 2.34 g, short-term DM = $198.34 \pm 4.35^*$ g ($p < 0.05$); long-term control = 458 ± 3.45 g, long-term DM = $350.39 \pm 3.43^*$ g ($p < 0.05$)]. The glucose levels in both urine and blood were more than 500 mg/dL and 300 mg/dL, respectively. The external appearances of the stomach were similar between control and diabetic rats in both periods. When the gross anatomy of the diabetic rat stom-

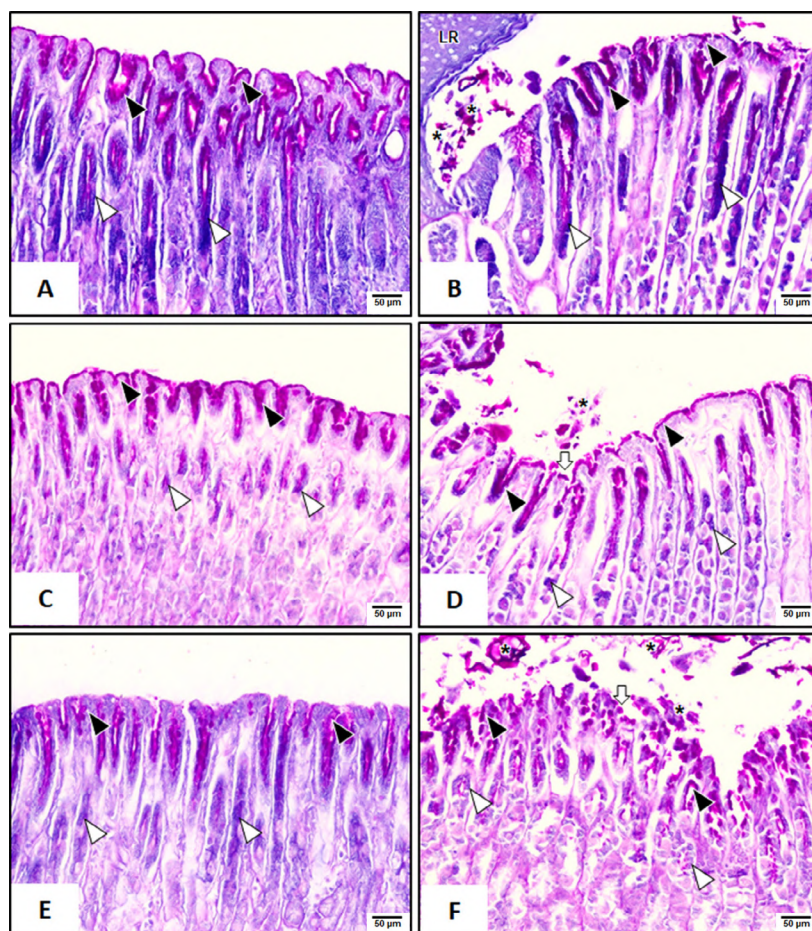


Fig. 1.- Light micrographs of gastric mucosa and gastric gland in the cardiac region (A-B), body region (C-D), and pyloric region (E-F) of short-term control (A, C, E) and short-term diabetic (B, D, F) rats. Positive reaction of PAS (black arrowheads); positive reaction PAS with strong Alcian blue (white arrowheads); limiting ridge (LR); slough tissue (asterisks); superficial erosion (white arrows). Combined Alcian blue-PAS staining. Scale bar = 50 μm .

ach was inspected visually, there was no apparent lesions or ulcers. The stomachs were divided into two sections of non-glandular and glandular parts, separated from each other by a limiting ridge. The non-glandular parts were shown as having whitish-brown mucosa, a translucent layer, and a thin wall. On the contrary, the glandular parts were represented by reddish mucosa and opaque, muscular, and thick wall.

Histopathological findings and mucin granule accumulations

The mucus-secreting cells were better visualized with Alcian-blue and PAS staining (Figs. 1-2), because the mucin granules were lost during HandE staining. In short-term DM rats, after Alcian-blue and PAS staining, greater sloughing of the gastric epithelium and gastric lumen and superficial erosions of the gastric glands were observed (Figs. 1B, 1D, 1F, 2B, 2D, 2F), compared to

those of the control rats (Figs. 1A, 1C, 1E, 2A, 2C, 2E). Staining with Alcian-blue and PAS can separate the deep magenta color of insoluble mucinogen granules of SMCs from the lighter magenta color of soluble mucinogen granules of MNCs. There was a significantly decreased percentage of mucin granule accumulation in both SMCs and MNCs in short- and long-term diabetic rats when compared with the control rats in the cardiac region (Figs. 1A-B, 2A-B), body region (Figs. 1C-D, 2C-D), and pyloric region (Figs. 1E-F, 2E-F), and Table 1. In addition, there were significantly decreased percentage of mucin granule accumulation in both SMCs and MNCs in long-term DM when compared to the short-term DM.

Ultrastructures of mucus-secreting cells

The mucus-secreting cells in this experiment represented secretory granules in both the supranuclear space and the apical surface of the cytoplasm.

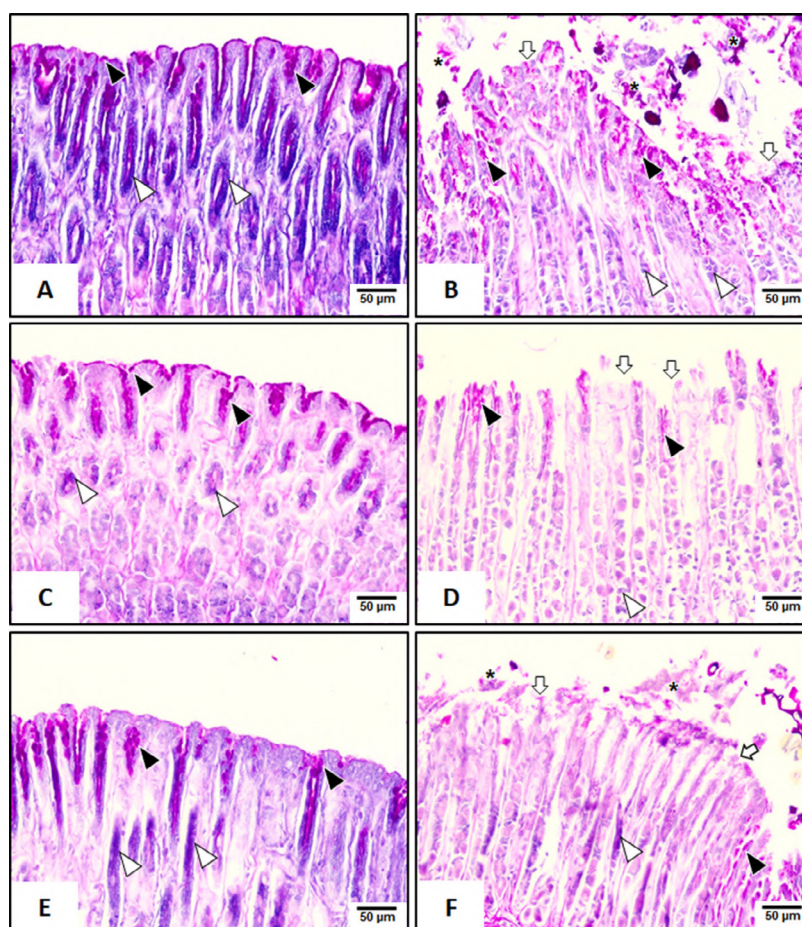


Fig. 2.- Light micrographs of gastric mucosa and gastric gland in the cardiac region (A-B), body region (C-D), and pyloric region (E-F) of long-term control (A, C, E) and long-term diabetic (B, D, F) rats. Positive reaction of PAS (black arrowheads); positive reaction PAS with strong Alcian blue (white arrowheads); slough tissue (asterisks); superficial erosion (white arrows). Combined Alcian blue-PAS staining. Scale bar = 50 μm.

Table 1. The percentage of mucin granule accumulations per area of SMCs and MNCs in all regions in both the short- and long-term periods.

Parameters			% Mucin granule accumulations per area (Mean ± SD)		
			Cardiac region	Body region	Pyloric region
SMCs	Short term	Control (n = 90)	29.20 ± 0.27	15.50 ± 0.84	20.03 ± 0.25
		DM (n = 90)	12.61 ± 0.16*	9.14 ± 0.97*	15.02 ± 0.15*
	Long term	Control (n = 90)	29.13 ± 0.18	18.47 ± 0.10	20.23 ± 0.24
		DM (n = 90)	8.93 ± 0.39**	3.59 ± 0.76**	1.58 ± 0.38**
MNCs	Short term	Control (n = 90)	29.73 ± 0.69	6.85 ± 0.10	9.52 ± 0.85
		DM (n = 90)	14.98 ± 0.14*	4.93 ± 0.11*	6.54 ± 0.15*
	Long term	Control (n = 90)	29.54 ± 0.13	6.86 ± 0.16	9.68 ± 0.14
		DM (n = 90)	5.59 ± 0.14**	2.34 ± 0.92**	0.96 ± 0.85**

*p<0.05; compared to the control rats in each gastric region in the same duration.

#p<0.05; compared to the short-term rats in each region.

Surface mucous cells (SMCs); Mucous neck cells (MNCs).

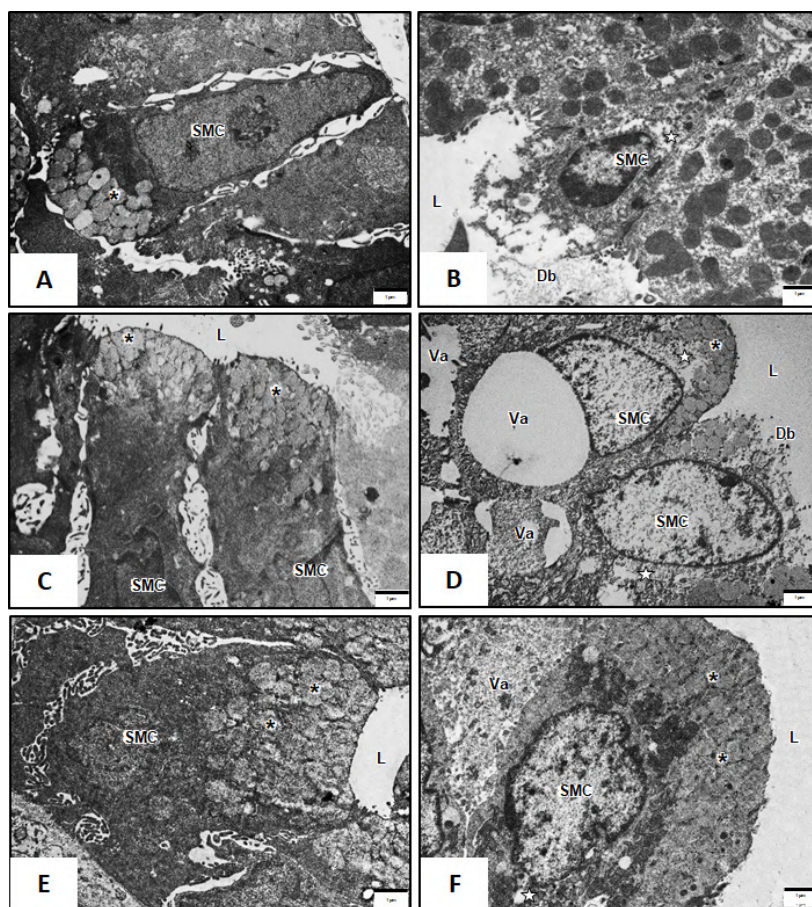


Fig. 3.- Transmission electron micrograph of surface mucous cells in the cardiac region (A-B), body region (C-D), and pyloric region (E-F) of short-term control (A, C, E) and short-term DM (B, D, F) rats. Surface mucous cell (SMC); lumen (L); vacuole (Va); debris (Db); black asterisks (mucin granules); electron lucent with unidentified structures (white stars). Scale bar = 1 μm.

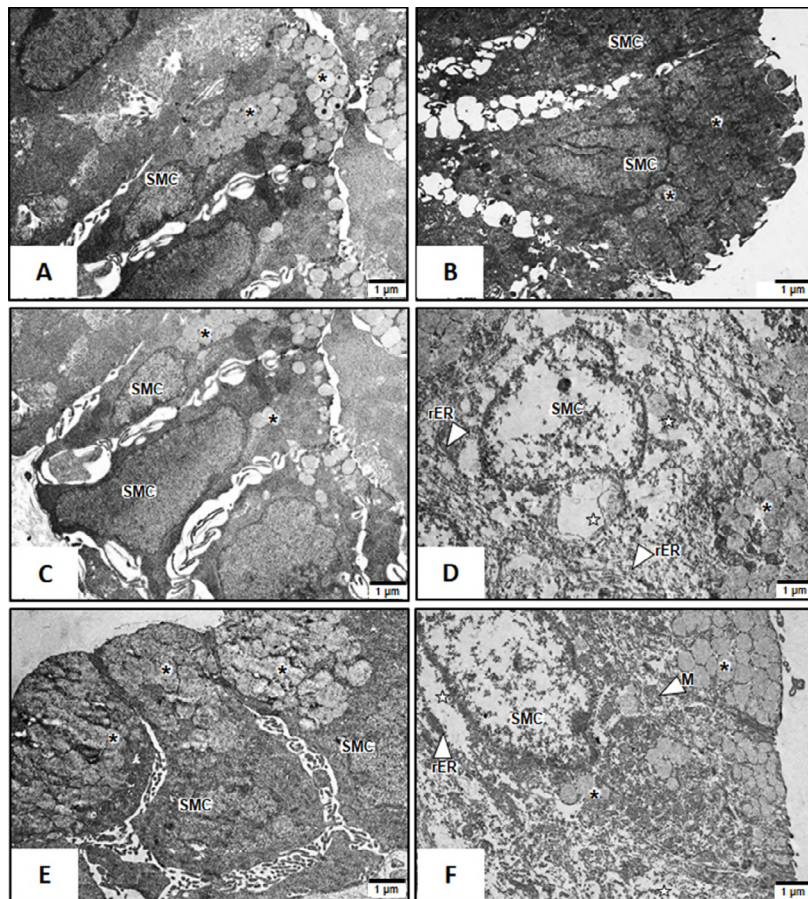


Fig. 4.- Transmission electron micrograph of surface mucous cells in the cardiac region (A-B), body region (C-D), and pyloric region (E-F) of long-term control (A, C, E) and long-term DM (B, D, F) rats. Surface mucous cell (SMC); rough endoplasmic reticulum (rER); black asterisks (mucin granules); rough endoplasmic reticulum (rER); mitochondria (M); electron lucent with unidentified structures (white stars). Scale bar = 1 μm.

Ultrastructures of surface mucous cells

In the control group, the mucous granule electron density varied in density at the apical area of SMCs (Figs 3A, 3C, 3E, 4A, 4C, 4E). SMCs in the apical areas of DM rats were swollen and damaged in short-term DM specimens. In addition, obvious cell debris and tiny fibrils (Figs. 3B, 3D), karyolitic nuclei (Fig. 3B), cytoplasmic vacuolation (Figs. 3D, 3F), and electron-dense granules at the apex were observed (Fig. 3F). Moreover, electron-lucent areas and unidentified structures were also demonstrated (Figs. 3B, 3D, 3F). In long-term DM specimens, destructive SMCs with degenerative nuclei (Figs. 4D, 4F) and mucous-filled cytoplasm were observed (Figs. 4B, 4D, 4F). Mucus from some SMCs was partially released (Fig. 4B). Cell organelles were destroyed (Fig. 4F). Dilated rER and electron-lucent regions and unidentified structures were also evident (Figs. 4D, 4F).

Ultrastructures of mucous neck cells

In the control group, bipartite secretory granules were present in MNCs (Figs. 5A, 5C, 5E, 6A, 6C, 6E). In the short-term DM group, cell swelling features of MNCs were observed (Figs. 5B, 5D). Numerous apical electron lucent mucous granules were present (Fig. 5D). In DM-MNCs, there was a large nucleolus in the euchromatin nucleus (Figs. 5B, 5D). This can be seen in the electron-lucent area, unidentified structures, and secondary lysosomes in their cytoplasm (Figs. 5B, 5D). Moreover, dilated rER was observed in the cytoplasm (Figs. 5B, 5D). In addition, a heterochromatin nucleus (Fig. 5F), and a dilated rER were found (Figs. 5B, 5D). The disappearance of mucous granules was seen (Fig. 5F). In long-term DM samples, MNCs with progressive swelling with nuclear chromatin condensation were also revealed (Fig. 6B). (Fig. 6B). Cytoplasmic organelles were degenerated, and electron-lucent areas were evident (Figs. 6B).

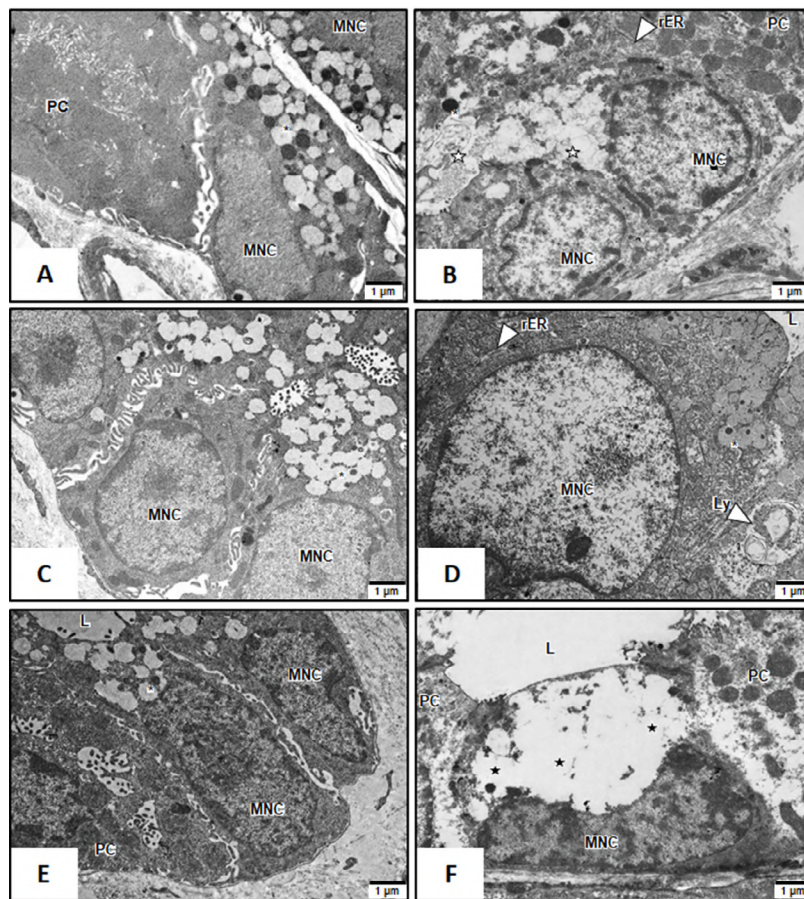


Fig. 5.- Transmission electron micrograph of mucous neck cells in the cardiac gland (A-B), gastric gland proper (C-D), and pyloric gland (E-F) of short-term control (A, C, E) and short-term DM (B, D, F) rats. Mucous neck cell (MNC); parietal cell (PC); lysosome (Ly); fibroblast (F); lumen (L); rough endoplasmic reticulum (rER); electron lucent with unidentified structures (white stars); mucin granules (black asterisks); disappeared mucin granules (black stars). Scale bar = 1 µm.

Secondary lysosomes, fragmented rER, and elongated mitochondria were also discovered (Figs 6D). Some MNC cells appeared to be characterized by the absence of mucin granules that previously existed in their cytoplasm (Fig. 6F).

DISCUSSION

The diabetic rats demonstrated diabetic symptoms such as polyuria, polydipsia, polyphagia, lethargy with sleep, inactivity with grooming, and unexplained weight loss, as well as abnormalities in both glucosuria and hyperglycemia, both of which were described in previous research (Baimai et al., 2020, 2021; Chookliang et al., 2021; Lerkdumnerkit et al., 2022). In this experiment, all rats were nourished with a standard diet and water. Therefore, there were no external factors, such as *H.pylori*, that affected the gastric epithelium. In addition, no other external stimuli, such as ethanol and NSAIDs were administered in this

study. Although there was no visible lesions or ulcers when the gross structure of the diabetic rat stomach was examined with the naked eye, superficial erosion of the epithelium lining every region of the stomach was visible under LM. It may be inferred that DM can damage SMCs. In the experimental results obtained by the LM, the evident damage was confirmed from the TEM images.

The appearance of the SMC in short-term DM showed superficial erosion; superficial erosion was found to be more common in uncontrolled long-term diabetes, as reported in 2019 (Raa-fat and Hamam, 2019). Superficial erosion was observed on the gastric mucosa in every region, which can indicate the disruption of epithelial tight junctions on surface epithelial cells (Harhaj and Antonetti, 2004; Groschwitz and Hogan, 2009; Rao, 2018). There had been several reports about the relationship between reactive oxygen species (ROS) and the disruption of epithelial

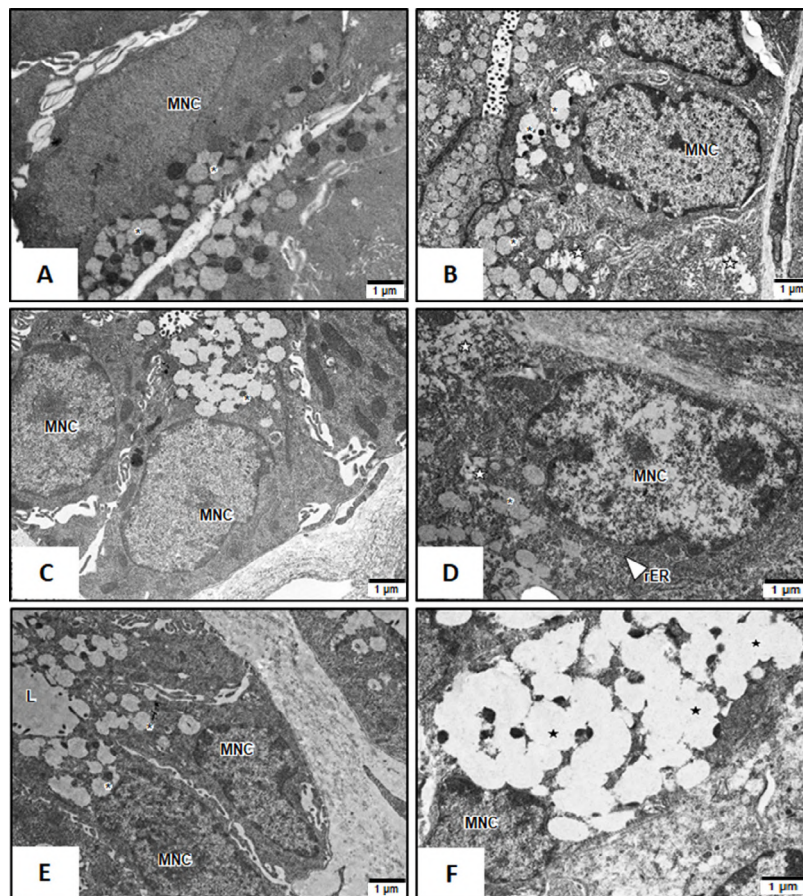


Fig. 6. - Transmission electron micrograph of mucous neck cells in the cardiac gland (A-B), gastric gland proper (C-D), and pyloric gland (E-F) of long-term control (A, C, E) and long-term DM (B, D, F) rats. Mucous neck cell (MNC); parietal cell (PC); lumen (L); electron lucent with unidentified structures (white stars); mucin granules (black asterisks); disappeared mucin granules (black stars). Scale bar = 1 μ m.

tight junctions (TJs) in the gastrointestinal tract (Harhaj and Antonetti, 2004; Groschwitz and Hogan, 2009; Rao, 2018). The epithelial surface consequently showed signs of cell debris, sloughing, and superficial erosion. SMCs were harmed by ongoing hyperglycemia and uncontrolled DM. Thus, the epithelium was shed as a result of the vicious cycle of DM.

Image analysis also revealed that mucin granules of SMCs and MNCs were significantly reduced in rats with short-term diabetes. When short-term and long-term DM were compared, the percentage of mucin granules gradually decreased. Accordingly, it can be possible that chronic hyperglycemia can worsen the severity of the disease. In addition, the electron microscopy results showed that vacuoles, fragmented rER, and destroyed organelles were found in SMCs and MNCs. Therefore, the mechanism of cell damage from DM can be explained as hyperglycemic con-

ditions destroying SMCs and MNCs via the ROS and apoptosis pathways.

Hyperglycemic blood can produce an excessive amount of sorbitol. A rise in the sorbitol content can cause water to enter the cells (Chung et al., 2003; Yan, 2018). Furthermore, sorbitol consumed a large amount of NADPH. The result was that DM generated excessive reactive oxygen species (ROS) production (Volpe et al., 2018; Ighodaro, 2018; Yaun et al., 2019). The cell membrane and organelles can be destroyed by ROS, which finally underwent fluid infusion. Vacuolated SMCs and MNCs were presented in both short- and long-term DM. Sustained hyperglycemia can change the mitochondria, causing them to malfunction. Then, ROS were produced, which triggered an apoptotic pathway via the recruitment of pro-caspase-9 (Krijnen et al., 2009). Caspase-9 promoted apoptosis by activating caspase-3. Chromatin condensation and pyknotic nuclei were

observed. SMCs and MNCs had pyknotic nuclei as a result of nuclear chromatin condensation. SMCs and MNCs that were destructive had dilated rER, damaged organelles, and unidentified features. Hyperglycemia condition can destroy SMCs by dilated rER in the cytoplasm and led to ER stress (Eizirik et al., 2008). Finally, apoptosis occurred in the cells. Sustained hyperglycemia can generate advanced glycation end products (AGE) (Singh et al., 2014; Saberzadeh-Ardestani et al., 2018). If AGEs were generated repeatedly, the ROS level would be increased and cause the DNA damages. Damaged DNA can stimulate the protein kinase C (PKC) pathway, which can also increase the ROS activities. Mucus-secreting cells found to dramatically decrease in short-term DM rats. Mucin granules in DM declined significantly over time, since ROS causes cell death with reduced mucin granules. Finally, during diabetic conditions, mucin granules were reduced in both cell types. From the DM group, it can be seen that the Golgi complex stores, packages, and concentrates proteins for export. If the organelle was destroyed, mucin within the Golgi disappears, which was consistent with the TEM images. DM can directly affect mucus-secreting cells. Consequently, stomach discomfort due to the mucosal protection damages can present in DM patients. Uncontrolled DM over a long period can increase the severity of destructive mucus-secreting cells and lead to GU, DU, and GERD.

CONCLUSION

STZ-induced diabetic rats showed both short-term and long-term destruction of the gastric mucosa and gastric gland structures under both LM and TEM. It was found that damage to SMCs and MNCs occurred in all regions of the stomach. Therefore, this is consistent with the occurrence of ulcers and GERD in diabetic patients presenting with gastrointestinal symptoms such as abdominal pain, nausea and vomiting, and stomach bleeding. Therefore, these DM model rats are a suitable model to explain how morphological changes develop over time. Thus, these findings provide insights and knowledge for future preventive medicine applications.

ACKNOWLEDGEMENTS

This research was supported by Chalermphrakiat Grant, Faculty of Medicine Siriraj Hospital, Mahidol University, Thailand.

REFERENCES

- BAIMAI S, JANTA S, LANLUA P, CHOOKLIANG A, NIYOMCHAN A, SRICHAROVENJ S (2020) Altered oligodendrocytes in spinal enlargements of streptozotocin diabetic rats. *Int J Morphol*, 38(6): 1606-1613.
- BAIMAI S, PHANICHAKUL P, LANLUA P, NIYOMCHAN A, SRICHAROVENJ S (2021) Modifications of adrenal gland ultrastructure in streptozotocin-induced diabetic model rats. *Int J Morphol*, 39(1): 109-115.
- BARRETT K, BROOKS H, BOITANO S, BARMAN S (2010) *Ganong's review of medical physiology 23rd edition*. Mc Graw Hill, New York.
- CHOOKLIANG A, LANLUA P, NIYOMCHAN A, SRICHAROVENJ S (2021) Small bronchiolar histopathological changes related to prolonged diabetes. *Int J Morphol*, 39(2): 371-377.
- CHUNG SSM, HO ECM, LAM KSL, CHUNG SK (2003) Contribution of polyol pathway of diabetes-induced oxidative stress. *J Am Soc Nephrol*, 14: S233-236.
- EIZIRIK D, CARDOZO AK, CNOP M (2008) The role of endoplasmic reticulum stress in diabetes mellitus. *Endocrine Rev*, 29(1): 42-61.
- GROSCWITZ KR, HOGAN SP (2009) Intestinal barrier function: Molecular regulation and disease pathogenesis. *J Allergy Clin Immunol*, 124(1): 3-22.
- HARHAJ NS, ANTONETTI DA (2004) Regulation of tight junctions and loss of barrier functions in pathophysiology. *IJBCB*, 36: 1206-1237.
- IGHODARO OM (2018) Molecular pathways associated with oxidative stress in diabetes mellitus. *Biomed Pharmacother*, 108: 656-662.
- KRIJNEN PA, SIMSEK S, NIESSEN HWM (2009) Apoptosis in diabetes. *Apoptosis*, 14: 1387-1388.
- KRISHNAN B, BABU S, WALKER J, WALKER AB, PAPPACHAN JM (2013) Gastrointestinal complications of diabetes mellitus. *WJD*, 4(3): 51-63.
- LERKDUMNERNKIT N, SRICHAROVENJ S, LANLUA P, NIYOMCHAN A, BAIMAI S, CHOOKLIANG A, PLAENGRIT K, PIANRUMLUK S, MANOONPOL C (2022) The effects of early diabetes on duodenal alterations in the rats. *Int J Morphol*, 40(2): 389-395.
- RAAFAT MH, HAMAN GG (2019) The possible role of bee venom on gastric fundic mucosa in streptozotocin induced diabetes mellitus in rats. A histological study. *EJH*, 42(4): 1029-1042.
- RAO R (2018) Oxidative stress-induced disruption of epithelial and endothelial junctions. *Front Biosci*, 13: 7210-7226.
- SABATINE MS (2020) *Pocket medicine*, 7th edition. Wolters Kluwer, Philadelphia.
- SABERZADEH-ARDESTANI B, KARAMZADEH R, BASIRI M, HAJIZADEH-SAFFAR E, FARHADI A, SHAPIRO J, TAHAMTANI Y, BAHARVAND H (2018) Type 1 diabetes mellitus: Cellular and molecular pathophysiology at a glance. *Cell J*, 20(3): 294-301.
- SINGH YP, BALI A, SINGH N, JAGGI AS (2014) Advanced glycation end products and diabetic complications. *Korean J Physiol Pharmacol*, 18(1): 1-14.
- VOLPE CMO, VILLAR-DELFINO PH, DOS ANJOS PMF, NOGUEIRA-MACHADO JA (2018) Cellular death, reactive oxygen species (ROS) and diabetic complications. *Cell Death Dis*, 9(2): 119.
- YAN LJ (2018) Redox imbalance stress in diabetes mellitus: Role of the polyol pathway. *Animal Model Exp Med*, 1(1): 7-13.
- YAUN T, YANG T, CHEN H, FU D, HU Y, WANG J, YUAN Q, YU H, XU W, XIE X (2019) New insights into oxidative stress and inflammation during diabetes mellitus-accelerated atherosclerosis. *Redox Biol*, 20: 247-260.